TRUE-AMPLITUDE WAVE-EQUATION MIGRATION

D. Amazonas, R. Aleixo, J. Schleicher and J. Costa

email: *daniela.amazonas@gmail.com*

keywords: *True-amplitude, wave-equation migration, split-step, FFD*

ABSTRACT

In heterogeneous media, standard one-wave wave equations only describe the kinematic parts of one-wave wave propagation correctly. For a correct description of amplitudes, the one-way wave equations must be modified. In vertically inhomogeneous media, the resulting true-amplitude one-way wave equations can be solved analytically. The corresponding amplitude modifications can be taken into account in split-step and Fourier finite difference migrations in such a way that they use these true amplitude one-way wave equations instead of the standard ones in order to implement a true amplitude wave equation migration for zero-offset data. Synthetic data examples demonstrate that the technique improves amplitude recovery in the migrated images.

INTRODUCTION

Many seismic migration methods, particularly those directly based on the wave equation, take only care of the kinematic aspects of the imaging problem (i.e., the position and structure of the seismic reflectors), while incorrectly treating the dynamics (amplitudes, related to the energy carried by the seismic wavefield). However, as post-migration AVO and AVA studies are becoming more and more important, the correct treatment of migration amplitudes becomes imperative.

In this work, we study wave-equation migration based on one-way wave equations. We are interested in such one-way wave equations that correctly describe not only the traveltime but also the amplitude of the resulting one-way waves. These one-way wave equations are referred to as true-amplitude one-way wave equations.

In homogeneous media, the product of the two differential operators of the two one-way wave equations, which are first-order differential equations, yields the differential operator of the full wave equation. The one-wave wave operators allow to separate the full wavefield into its components traveling in different directions. Generally, the factorization is used to split the wavefield into its up- and downgoing parts. In this form, the one-way wave equations are useful in modeling and, principally, in migration.

In a homogeneous medium, traveltimes and amplitudes of the one-way waves, i.e., the solutions of the so-obtained one-way wave equations are identical to those of the solution of the full wave equation. However, in inhomogeneous media, the use of the same one-way wave equation leads to different amplitudes than those of the solution of the full wave equation.

Recently, Zhang et al. (2003) showed how to modify the differential operators of the one-way wave equations such that, in zero-order ray approximation, the amplitudes are the same as those governed by the full wave equation. They have shown how to use the modified one-way wave equations in finite-difference true-amplitude common-shot wave-equation migration. Melo et al. (2006) transferred this idea to poststack (zero-offset) phase-shift migration (Gazdag, 1978) using the true-amplitude one-way wave equations. They solved these equations analytically and showed that amplitude correction can be achieved by a simple factor to be applied at each depth step. Here, we generalize their ideas to poststack split-step (Stoffa et al., 1990) and Fourier finite-difference (Ristow and Rühl, 1994) migration using the true-amplitude one-way wave equations.

METHOD

We consider the two-dimensional acoustic wave equation

$$\mathcal{L}u = \nabla^2 u - \frac{1}{c^2}\frac{\partial^2 u}{\partial t^2} = 0 \,, \tag{1}$$

where $u = u(x, z, t)$ is the seismic wave field, and where the propagation velocity c may be constant or depend on one or two spatial coordinates.

Ray equations

Let us start with the simple case of a velocity that depends only on depth, i.e., $c = c(z)$. In this case, the solution of equation (1) can be found using its Fourier transform in time as well as in the horizontal coordinate, viz.

$$\frac{\partial^2 u}{\partial z^2} + \omega^2 p_z^2 u = 0 \,, \tag{2}$$

where

$$p_z = \frac{k_z}{\omega} = \pm\frac{1}{c(z)}\sqrt{1 - (c(z)p_x)^2} \,, \tag{3}$$

where k_x is the wavenumber component relative to coordinate x and

$$k_z = \pm\sqrt{\frac{\omega^2}{c^2} - k_x^2} = \pm\frac{\omega}{c}\sqrt{1 - \frac{(ck_x)^2}{\omega^2}} \,. \tag{4}$$

The representation in the rightmost part of equation (4) was chosen so that the upper sign describes downward propagation while the lower sign describes upward propagation.

Substitution of the ray ansatz

$$u(z, \omega) = A(z)\exp\{i\omega\tau(z)\} \,, \tag{5}$$

where A is amplitude and τ is traveltime, in the Helmholtz equation (2) leads to the eikonal and transport equations

$$\left(\frac{\partial\tau}{\partial z}\right)^2 = p_z^2 \quad : \quad \frac{\partial\tau}{\partial z} = \pm p_z \,, \tag{6}$$

and

$$2\frac{\partial\tau}{\partial z}\frac{\partial A}{\partial z} + \frac{\partial^2\tau}{\partial z^2}A = 0 \,. \tag{7}$$

Taking the derivative of the eikonal equation (6) with respect to z using Snell's law $\frac{\partial p_x}{\partial z} = 0$, we find

$$\frac{\partial^2\tau}{\partial z^2} = \pm\frac{\partial p_z}{\partial z}. \tag{8}$$

Substitution of this result in the transport equation (7) yields

$$\pm\left[2p_z\frac{\partial A}{\partial z} + \frac{\partial p_z}{\partial z}A\right] = 0 \,. \tag{9}$$

While the vertical derivative of p_z can be determined from equation (3) as

$$\frac{\partial p_z}{\partial z} = -\frac{1}{p_z c^3}\frac{\partial c}{\partial z}, \tag{10}$$

it will be more convenient below to recognize that for $p_z \neq 0$, equation (9) is equivalent to

$$\frac{\partial A}{\partial z} + \frac{1}{2}\frac{\partial\ln(p_z)}{\partial z}A = 0 \,. \tag{11}$$

In the above expressions, the upper and lower signs refer to the down- and upgoing waves, respectively. Note that both waves, independently of their predominant propagation direction, must satisfy the same transport equation.

TRUE-AMPLITUDE ONE-WAY WAVE EQUATIONS

For a constant medium velocity, it is easy to verify that the Helmholtz equation (2) can be factorized as

$$\left[\frac{\partial}{\partial z} \pm ik_z\right]\left[\frac{\partial}{\partial z} \mp ik_z\right] u = \mathcal{L}_0^{\pm}\mathcal{L}_0^{\mp} u = \frac{\partial^2 u}{\partial z^2} + k_z^2 u = 0 \,, \tag{12}$$

where

$$\mathcal{L}_0^{+} = \left[\frac{\partial}{\partial z} + ik_z\right] \,, \quad \mathcal{L}_0^{-} = \left[\frac{\partial}{\partial z} - ik_z\right] \tag{13}$$

are the differential operators of the one-way wave equations. Once we fix the sign of k_z according to

$$k_z = \mathrm{sgn}(\omega)\sqrt{\frac{\omega^2}{c^2} - k_x^2} = \frac{\omega}{c}\sqrt{1 - \frac{(ck_x)^2}{\omega^2}} \,, \tag{14}$$

$\mathcal{L}_0^{+}$ and $\mathcal{L}_0^{-}$ describe downgoing and upgoing waves, respectively. Therefore, any solution of

$$\mathcal{L}_0^{+} u^{+} = 0 \qquad \text{or} \qquad \mathcal{L}_0^{-} u^{-} = 0 \tag{15}$$

is also a solution of the Helmholtz equation (2). This motivates the use of one-wave wave equations in migration, where only downward propagation is required.

Let us now look for solutions of the one-way wave equations (15) of the type

$$u^{\pm}(z,\omega) = A^{\pm}(z)\exp\{i\omega\tau^{\pm}(z)\} \,. \tag{16}$$

The resulting eikonal and transport equations read

$$\frac{\partial \tau^{\pm}}{\partial z} = \pm p_z \,, \tag{17}$$

$$\frac{\partial A^{\pm}}{\partial z} = 0 \,. \tag{18}$$

We see that the eikonal equations (6) and (17) are identical, which reflects the well-known fact that even in homogeneous media, the kinematics of the up- and downgoing waves are correctly described by the one-wave wave equations. However, comparing the transport equations (7) and (18), we see that they are identical only in homogeneous media, where $\dfrac{\partial c}{\partial z} = 0$ and consequently $\dfrac{\partial p_z}{\partial z} = 0$

Therefore, for the one-way wave equations to correctly describe the amplitudes of the up- and downgoing waves, at least up to zero-order ray theory, they need to be modified (Zhang et al., 2003). The simplest way to do so is by adding a new term $\alpha^{\pm}$ to the one-way wave operators $\mathcal{L}_0^{\pm}$. Doing so results in the modified equations

$$\left[\frac{\partial}{\partial z} \pm ik_z + \alpha^{\pm}\right] u = 0 \,. \tag{19}$$

Searching for solutions of the ray type in equation (16), we find the eikonal and transport equations

$$\frac{\partial \tau^{\pm}}{\partial z} = \pm p_z \,, \tag{20}$$

$$\frac{\partial A^{\pm}}{\partial z} + \alpha^{\pm} A^{\pm} = 0 \,. \tag{21}$$

Comparing these equations with those obtained for the full wave equation [equations (6) and (7)], it is easy to recognize that the eikonal equations are still the same. For the transport equations to be identical, both $\alpha^{\pm}$ need to be chosen as

$$\alpha^{\pm} = -\frac{1}{2}\frac{1}{p_z^2 c^3}\frac{\partial c}{\partial z} = \frac{1}{2}\frac{\partial}{\partial z}\ln(p_z) \,. \tag{22}$$

Thus, the true-amplitude one-way wave equations read (Zhang et al., 2003)

$$\left\{\frac{\partial}{\partial z} \mp i\omega p_z - \frac{1}{2}\frac{1}{p_z^2 c^3}\frac{\partial c}{\partial z}\right\} u = 0 \,, \tag{23}$$

or, more conveniently,

$$\left\{ \frac{\partial}{\partial z} \mp i\omega p_z + \frac{1}{2} \frac{\partial}{\partial z} \ln(p_z) \right\} u = 0 \; . \tag{24}$$

By construction, these equations describe up- and downgoing waves that possess, in zero-order ray theory approximation, the same amplitudes and traveltimes as those described by the full wave equation.

SPLIT-STEP MIGRATION

Split-step migration was developed by Stoffa et al. (1990) to migrate stacked seismic data in two or three dimensions. This migration method is implemented in the $\omega - x$ and $\omega - k$ domain and allow us to use for small lateral variations in velocity around the reference velocity in the jth layer, c_j.

Using the notation of last section, we can deduce the split-step approximation from the relation

$$\frac{i\omega}{c}\sqrt{1+\frac{c^2}{\omega^2}\frac{\partial^2}{\partial x}} = \frac{i\omega}{c_j}\sqrt{1+\frac{c_j^2}{\omega^2}\frac{\partial^2}{\partial x}} + \left[\frac{i\omega}{c}\sqrt{1+\frac{c^2}{\omega^2}\frac{\partial^2}{\partial x}} - \frac{i\omega}{c_j}\sqrt{1+\frac{c_j^2}{\omega^2}\frac{\partial^2}{\partial x}} \right] , \tag{25}$$

where now $c = c(x, z)$.

Expanding the first of the square roots inside the brackets in a Taylor series up to first order in c around c_j, we obtain

$$\frac{i\omega}{c}\sqrt{1+\frac{c^2}{\omega^2}\frac{\partial^2}{\partial x}} \approx \frac{i\omega}{c_j}\sqrt{1+\frac{c_j^2}{\omega^2}\frac{\partial^2}{\partial x}} + \frac{i\omega}{c_j}\left(\frac{c_j}{c} - 1\right) \; . \tag{26}$$

Substituting this approximation in the one-way wave equation, we have an equation with lateral-variation correction

$$\frac{\partial U(k_x, z, \omega)}{\partial z} = \frac{i\omega}{c_j}\left[\sqrt{1 - \frac{k_x^2 c_j^2}{\omega^2}} + \frac{c_j}{c} - 1 \right] P(k_x, z, \omega) \; . \tag{27}$$

The solution of equation (27) can be put in the form

$$U'(k_x, z_{j+1}, \omega) = U(k_x, z_j, \omega) \exp\left\{ \frac{i\omega}{c_j}\sqrt{1 - \left(\frac{k_x\, c_j}{\omega}\right)^2}\,(z_{j+1} - z_j) \right\} , \tag{28}$$

$$U(x, z_{j+1}, \omega) = U'(x, z_{j+1}, \omega) \exp\left\{ i\omega \left(\frac{1}{c} - \frac{1}{c_j}\right)(z_{j+1} - z_j) \right\} , \tag{29}$$

where $U'(x, z_{j+1}, \omega)$ is the inverse Fourier transform of $U'(k_x, z_{j+1}, \omega)$.

COMPLEX PADÉ FOURIER FINITE DIFFERENCE MIGRATION

Following the methodology proposed by Ristow and Rühl (1994), Amazonas et al. (2007) rederived the FFD algorithm using the complex Padé approximation (Millinazzo et al., 1997).

Ristow and Rühl's FFD method can be obtained by the real approximation of the square root in brackets in equation (25) (Ristow and Rühl, 1994),

$$\sqrt{\frac{\omega^2}{c^2} + \frac{\partial^2}{\partial x^2}} \approx \sqrt{\frac{\omega^2}{c_r^2} + \frac{\partial^2}{\partial x^2}} + \frac{\omega}{c_r}(p-1)\left\{ 1 + \frac{\frac{c^2}{\omega^2}\frac{\partial^2}{\partial x^2}}{a_1 + b_1 \frac{c^2}{\omega^2}\frac{\partial^2}{\partial x^2}} + \frac{\frac{c^2}{\omega^2}\frac{\partial^2}{\partial x^2}}{a_2 + b_2 \frac{c^2}{\omega^2}\frac{\partial^2}{\partial x^2}} + ... \right\} , \tag{30}$$

where $c_r \leq c$ is a constant reference velocity, and where the coefficients a_n, b_n, $n = 1, 2, 3, ...$ depend on $p = c_r/c$ and $c = c(x, z)$. Equation (30) can be interpreted as a real Padé approximation.

Amazonas et al. (2007) showed that a more stable FFD method uses the corresponding complex Padé approximation, represented by the following expression

$$p\sqrt{1+\frac{c^2}{\omega^2}\frac{\partial^2}{\partial x_1^2}} \approx \sqrt{1+\frac{c_r^2}{\omega^2}\frac{\partial^2}{\partial x_1^2}} + C_0(p-1) + \sum_{n=1}^{N} \frac{A_n p(1-p)\frac{c^2}{\omega^2}\frac{\partial^2}{\partial x_1^2}}{1 + \sigma B_n \left(\frac{c}{\omega}\right)^2 \frac{\partial^2}{\partial x_1^2}} \; , \tag{31}$$

where C_0, A_n, and B_n are the complex Padé coefficients determined from the real ones by a rotation of the branch cut of the complex square root (Amazonas et al., 2007). While the correct approximation requires that parameter σ should be $\sigma = 1 + p + p^2$, numerical experiments showed that the heuristic value $\sigma = 1 + p^3$ yields a more accurate slowness curve.

Using the complex Padé FFD approximation in the kinematic part of the one way wave equation, we have an equation with lateral variation correction

$$\frac{\partial U(k_x, z, \omega)}{\partial z} = \frac{i\omega}{c_j} \left[\sqrt{1 - \frac{k_x^2 c_j^2}{\omega^2}} + C_0(p-1) + \sum_{n=1}^{N} \frac{A_n p(1-p) X^2}{1 + \sigma B_n X^2} \right] P(k_x, z, \omega) \; . \tag{32}$$

To find the FFD contribution we have to solve a finite-difference scheme.

TRUE-AMPLITUDE MIGRATION

We now use the true-amplitude one-way wave equations to introduce amplitude control into split-step phase-shift plus interpolation (SSPSPI) and complex-Padé FFD migrations. Thus, we need to solve the true-amplitude one-way wave equation

$$\left\{ \frac{\partial}{\partial z} - i\omega p_z - \frac{1}{2} \frac{d}{dz} \ln(p_z) \right\} u = 0 \; , \tag{33}$$

where p_z is still given by equation (3).

Following Melo et al. (2006), the differential equation (33) can be solved by separation of variables. Integration from initial depth z_0 to final depth z_f yields the expression for the wavefield u_f at depth level z_f,

$$\begin{aligned} u_f &= u_0 \exp \left\{ i\omega \int_{z_0}^{z_f} p_z \, dz + \int_{z_0}^{z_f} \frac{1}{2} \frac{d}{dz} \ln(p_z) dz \right\} \\ &= u_0 \exp \left\{ i\omega \int_{z_0}^{z_f} p_z \, dz \right\} \exp \left\{ \int_{z_0}^{z_f} \frac{1}{2} \frac{d}{dz} \ln(p_z) dz \right\} \; . \end{aligned} \tag{34}$$

Note that the first exponential term in equation (34) is nothing else but the phase correction term of conventional Gazdag migration. The second exponential term gives rise to the amplitude correction in inhomogeneous media, resulting from the correction term α in the true-amplitude one-way wave equation (33).

Let us now suppose that the medium has a vertically varying velocity, i.e., $c = c(z)$. To solve the integral in the first exponential term, we again divide the depth interval $[0, z]$ in N_z subintervals $I_j = \{z | z_j < z < z_{j+1};\ j = 0, 1, 2, ..., N_z - 1\}$. We then apply the solution (34) to each single layer, i.e., $z_0 = z_j$ and $z_f = z_{j+1}$. Denoting the the wavefield at depth z_j as $u_j = u(k_x, z_j, \omega)$, we may thus write

$$\begin{aligned} u_{j+1} &= u_j \exp \left\{ i\omega \int_{z_j}^{z_{j+1}} p_z \, dz + \int_{z_j}^{z_{j+1}} \frac{1}{2} \frac{d}{dz} \ln(p_z) dz \right\} \\ &= u_j \sqrt{\frac{p_{z_{j+1}}}{p_{z_j}}} \exp \left\{ \int_{z_j}^{z_{j+1}} (i\omega p_z) dz \right\} \; . \end{aligned} \tag{35}$$

Thus, the true-amplitude expression for wave-equation migration reads (Melo et al., 2006)

$$u_{j+1} = u_j \sqrt{\frac{p_{z_{j+1}}}{p_{z_j}}} \exp \left\{ i\omega \bar{p}_z (z_{j+1} - z_j) \right\} \; , \tag{36}$$

where p_{z_j} and $p_{z_{j+1}}$ denote the vertical slowness vector components at the top and bottom of the current layer, while $\bar{p}_z$ is the mean value of the function $p_z(z)$ in interval $[z_j, z_{j+1}]$. For practical purposes, $\bar{p}_z$ must be approximated by some reasonably chosen value based on the known values of p_z. For example, pure phase-shift migration uses the approximation $\bar{p}_z = p_{z_j}$.

Peak	SSPSPI amplitude gain (%)	FFD amplitude gain (%)
1	38.46	18.66
2	46.17	28.08
3	42.49	18.60
4	53.35	24.71
5	48.16	25.89
6	28.66	12.77
7	44.15	26.98
8	37.01	20.59
9	61.50	26.72
10	22.24	11.05
11	44.15	17.88
12	63.31	36.47
13	48.01	18.99
14	50.60	25.11
15	53.84	26.94
16	72.60	28.79

Table 1: Relative gain of the peaks as numbered in Figures 2 and Figure 4.

Clearly, the first approximations to true-amplitude split-step and FFD migrations are obtained by using the corresponding square-root approximations (26) and (31) for p_z in the phase term while keeping the amplitude correction unchanged. Future studies will include the use of these approximations also for the amplitude correction factor.

NUMERICAL EXPERIMENTS

To test the numerical properties of the amplitude correction for SSPSPI and complex-Padé FFD migration, we applied the proposed algorithms with and without amplitude correction to synthetic data from the SEG/EAGE salt model (Aminzadeh et al., 1995).

SSPSPI migration

For the SSPSPI migrations, we used a set of 20 reference velocities chosen between the minimum and maximum velocity at the current depth level according to the entropy criterion of Bagaini et al. (1995). Figure 1 shows the migrated sections obtained by the SSPSPI (top) and true-amplitude SSPSPI (bottom) algorithms. We see that the true-amplitude algorithm produces a clearer image of the reflectors. Particularly the bottom of the salt and subsalt reflectors have increased amplitudes. The colored lines indicate locations for trace-to-trace comparisons.

To evaluate the result more quantitatively, we have extracted three traces from these sections, at the horizontal positions of $x = 3901.44$ m (blue line in the sections), $x = 7863.84$ m (green line) and $x = 11545.82$ m (red line). These locations were chosen to represent three different areas of the model. The leftmost position (blue line) is in the purely sedimentary region, the central position (green line) marks the central part of the salt body, and the rightmost position (red line) cuts the right wedge of the salt body.

Figure 2 compares these three traces as obtained with the conventional (red) and true-amplitude (blue) algorithm. The general amplitude enhancement is clearly visible. However, we note that not all reflectors are enhanced by the same amount. The relative gain of the peaks as numbered in Figure 2 is quantified in Table 1. These values corroborate our impression that the main amplitude enhancement is achieved for the bottom-of-salt and subsalt reflectors.

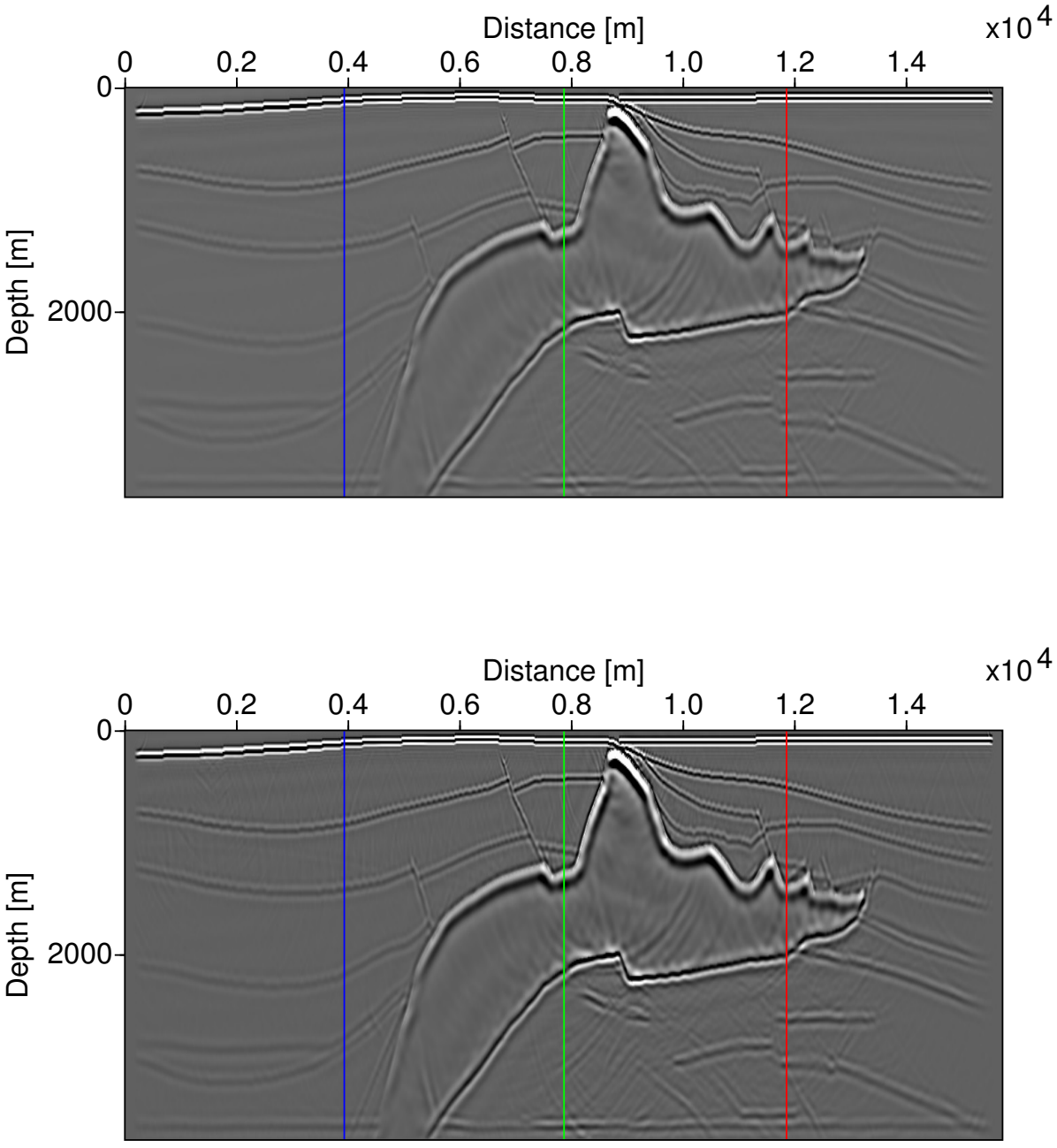

Figure 1: Migrated sections using SSPSPI depth migration. Top: Conventional algorithm; Bottom: true-amplitude algorithm.

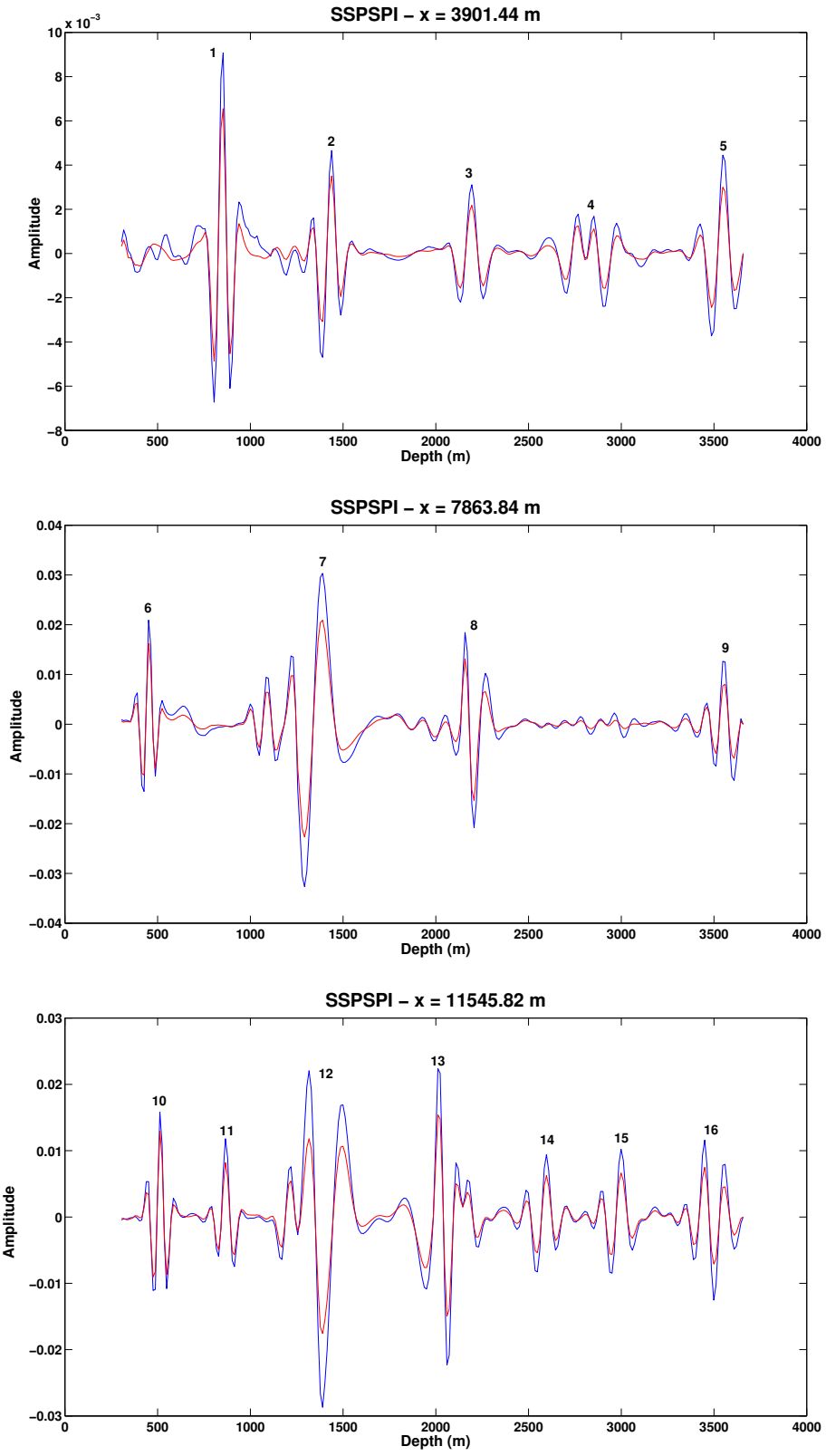

Figure 2: Migrated traces using SSPSPI depth migration at the horizontal positions of $x = 3901.44$ m (top), $x = 7863.84$ m (center) and $x = 11545.82$ m (bottom) as obtained with the conventional (red) and true-amplitude (blue) algorithm.

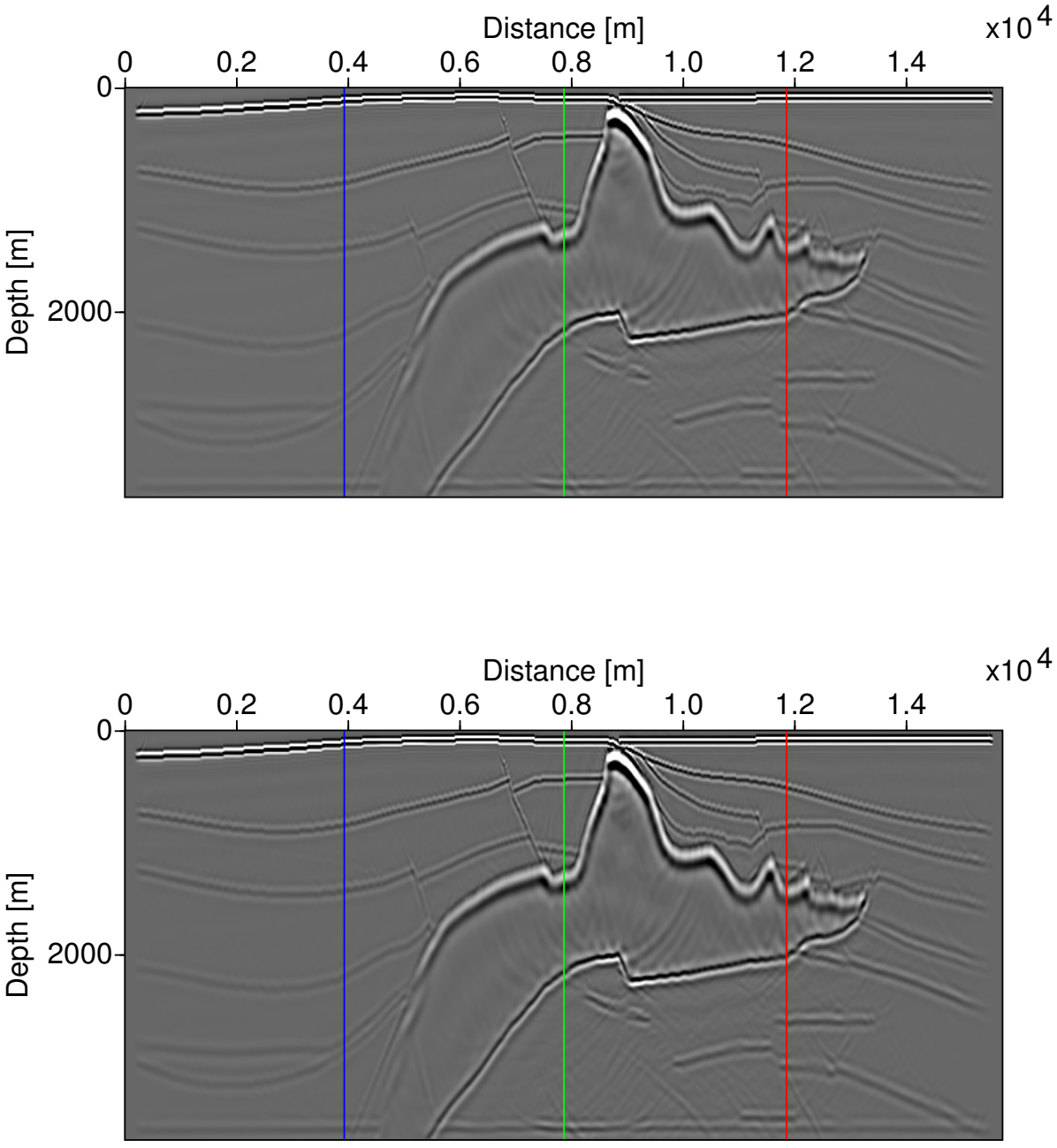

Figure 3: Migrated sections using complex-Padé FFD depth migration. Top: conventional algorithm; Bottom: true-amplitude algorithm.

Complex Padé FFD migration

Our FFD migration used the smallest model velocity at the present depth level as the reference velocity v_r. Figure 3 shows the migrated sections obtained by the conventional (top) and true-amplitude (bottom) complex-Padé FFD migration algorithms. As expected, the FFD algorithms produce a better image than the corresponding SSPSPI algorithms. The comparison between the conventional and true-amplitude FFD algorithms provides a similar picture as that for the SSPSPI migration. We see enhanced reflector amplitudes, particularly at the bottom-of-salt and subsalt reflectors.

As before, we extracted three traces from these sections for a trace-by-trace comparison at the horizontal positions of $x = 3901.44$ m (blue line in the sections), $x = 7863.84$ m (green) and $x = 11545.82$ m (red). These traces from the conventional (red) and true-amplitude algorithms (blue) are compared in Figure 4. As in the SSPSPI case, we see a general enhancement of the amplitudes, however not uniform. The relative amplitudes gains are also presented in Table 1. We note that the general distribution of which reflectors experience the strongest enhancement is very similar to the one of SSPSPI migration. However, the overall amplitude enhancement in the FFD algorithm is about 50% reduced.

The reason for this different amplitude behavior is the fact that the amplitude correction for the FFD algorithm is done using the reference velocity, which is the lowest velocity at the current depth level, while the SSPSPI algorithm effectively uses reference velocities much closer to the true velocity. Moreover, by interpolating wavefields after the amplitude correction, the SSPSPI algorithm even carries information about the lateral velocity variations over to the amplitudes.

CONCLUSION

For a correct description of amplitudes in wave-equation depth migration, the one-way wave equations must be modified (Zhang et al., 2003). The modified true-amplitude one-way wave equations can be solved exactly for vertically inhomogeneous media (Melo et al., 2006). In this work, we have implemented the resulting amplitude correction factor in split-step phase-shift plus interpolation (SSPSPI) and complex Padé Fourier finite difference (CPFFD) migration algorithms, so as to carry out a true-amplitude wave-equation migration for poststack (zero-offset) data. Synthetic data examples demonstrate that the technique improves amplitude recovery in the migrated images. In the SEG/EAGE salt model, the main amplitude enhancement was achieved for the bottom-of-salt and subsalt reflectors. The relative gain in amplitudes was significantly higher for SSPSPI than for CPFFD migration.

In this work, we investigated the most basic approximations to true-amplitude SSPSPI and CPFFD migrations, obtained by using their respective square-root approximations only in the phase term while keeping the simple $v(z)$-amplitude correction unchanged. This explains the better amplitude recovery in SSPSPI migration, which involves a wavefield interpolation at each lateral position after the propagation and amplitude correction. In this way, it takes lateral velocity variations into account even in the amplitudes. On the other hand, in CPFFD migration the amplitude correction is simply carried out with the reference velocity, thus ignoring lateral velocity variations. Future studies will include the use of the respective SSPSPI and CPFFD square-root approximations also for the amplitude correction factor.

ACKNOWLEDGMENTS

This work was kindly supported by the Brazilian research agencies CNPq and FAPESP (proc. 06/04410-5), as well as Petrobras and the sponsors of the *Wave Inversion Technology (WIT) Consortium*.

REFERENCES

Amazonas, D., Costa, J. C., Schleicher, J., and Pestana, R. (2007). Wide-angle FD and FFD migration using complex Padé approximations. *Geophysics*, 72(6):S215–S220.

Aminzadeh, F., Burkhard, N., Kunz, T., Nicoletis, L., and Rocca, F. (1995). 3-D modeling project: 3rd report. *The Leading Edge*, 14(2):125–128.

Bagaini, C., Bonomi, E., and Pieroni, E. (1995). Data parallel implementation of 3-D PSPI. In *65th Ann. Internat. Mtg., SEG, Expanded Abstracts*, pages 188–191.

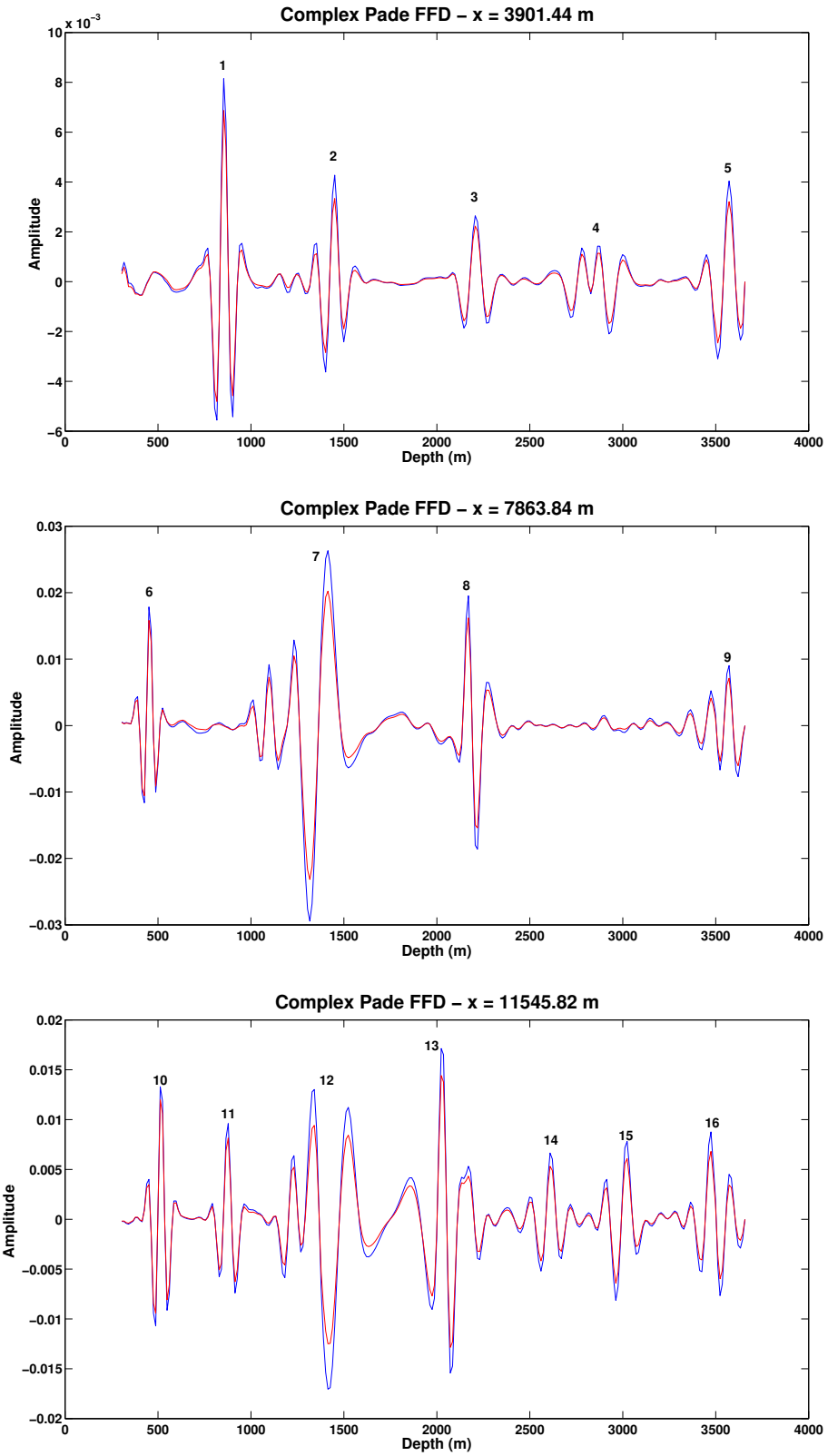

Figure 4: Migrated traces using complex Padé FFD depth migration at the horizontal positions of $x = 3901.44$ m (top), $x = 7863.84$ m (center) and $x = 11545.82$ m (bottom) as obtained with the conventional (red) and true-amplitude (blue) algorithm.

Gazdag, J. (1978). Wave equation migration with the phase-shift method. *Geophysics*, 43(07):1342–1351.

Melo, G., Schleicher, J., and Novais, A. (2006). Poststack true amplitude wave-equation migration. *Annual WIT Report*, 10:145–158.

Millinazzo, F. A., Zala, C. A., and Brooke, G. H. (1997). Square-root approximations for parabolic equation algorithms. *J. Acoust. Soc. Am.*, 101(2):760–766.

Ristow, D. and Rühl, T. (1994). Fourier finite-difference migration. *Geophysics*, 59(12):1882–1893.

Stoffa, P. L., Fokkema, J. T., Freire, R. M., and Kissinger, W. P. (1990). Split-step Fourier migration. *Geophysics*, 55(4):410–421.

Zhang, Y., Zhang, G., and Bleistein, N. (2003). True amplitude wave equation migration arising from true amplitude one-way wave equations. *Inverse Problems*, 19:1113–1138.